

## DESIGN STUDY ON 0.3-NM PAL XFEL

J. S. Oh, I. S. Ko, and W. Namkung, PAL/POSTECH, Pohang 790-784, Korea  
Y. Kim, DESY, D-22603 Hamburg, Germany

### Abstract

PAL is operating a 2.5-GeV electron linac as a full-energy injector to the PLS storage ring. The PAL linac can be converted to a SASE-XFEL facility (PAL XFEL) that supplies coherent X-rays down to 0.3-nm wavelength. It requires a 3-GeV driver linac and a 60-m long in-vacuum undulator with a 3-mm gap and a 12.5-mm period to realize a hard X-ray SASE-FEL. The linac should supply highly bright beams with emittance of 1.5 mm-mrad, a peak current of 4 kA, and a low energy spread of 0.02%. FEL performance is very sensitive to electron beam parameters. The beam quality is degraded along the undulator trajectory due to the energy loss and the wake field. Also the FEL gain is reduced by errors in the undulator fields and beam trajectories. The preliminary design details for the 0.3-nm PAL-XFEL are presented with parametric analysis.

### INTRODUCTION

PAL operates a 2.5-GeV electron linac, the 3<sup>rd</sup> largest in the world, as a full-energy injector to the PLS storage ring [1]. The PAL 2.5-GeV linac can be converted to an X-ray free electron laser (XFEL) facility driven by a self-amplified spontaneous emission (SASE) mode, which supplies coherent X-rays down to 0.3-nm wavelength. The undulator length has to be less than 60 m considering available site area and reasonable cost. Table 1 shows the comparison of single bunch specifications between the PLS linac and PAL XFEL. The linac should supply highly bright 3-GeV beams of which emittance of 1.5 mm-mrad, a peak current of 4 kA, and a low energy spread of 0.02% [2]. Normalized emittance should be improved 100 times, which requires a low emittance gun and high gradient acceleration at low energy region to preserve the emittance. A suitable bunch compression technique is important to realize the high peak current. The performance and stability of the 2.5-GeV linac is also challenging to meet the strict SASE requirements.

Table 1: Bunch specifications of PLS linac and XFEL

| Parameter            | PLS Linac         | PAL XFEL          |
|----------------------|-------------------|-------------------|
| Beam energy          | 2.5 GeV           | 3.0 GeV           |
| Normalized emittance | 150 $\mu\text{m}$ | 1.5 $\mu\text{m}$ |
| FWHM bunch length    | 13 ps             | 0.23 ps           |
| RMS energy spread    | 0.26%             | 0.02%             |
| Bunch charge         | 0.43 nC*          | 1.0 nC            |
| Peak current         | 33 A*             | 4 kA              |
| Repetition rate      | 10 Hz             | 60 Hz             |

\* 2-A gun current and 62% transmission

### 0.3-NM PAL XFEL

The fundamental radiation wavelength  $\lambda_x$  of an undulator is given by

$$\lambda_x = \frac{\lambda_u}{2\gamma^2} (1 + K^2/2), \quad \gamma = E_o/0.511, \quad K = 0.934B_u\lambda_u,$$

where  $E_o$  is the beam energy in MeV,  $B_u$  is the peak magnetic field of the undulator in Tesla, and  $\lambda_u$  is the undulator period in cm. Either a short-period undulator or a high-energy beam can provide short-wave radiation. A short-period undulator is preferred for a compact FEL machine. It is important to keep a reasonably large undulator parameter  $K$  to obtain a short saturation length. An in-vacuum mini-gap undulator can meet this requirement. This idea was introduced by T. Shintake for the SCSS project at SPring-8 [3].

Each curve in Fig. 1 shows the undulator parameters of the 0.3-nm PAL XFEL for saturation lengths of 40, 50, 60 m and beam energy of 2.5, 3.0, 3.5 GeV, respectively. The possible solution that is reasonably economic, to meet the saturation length of 50 m, is to use an undulator with a 3-mm gap, 12.5-mm period and a 3-GeV beam. For the saturation length of 50 m, the largest gap is 3.4 mm with 16-mm period at the beam energy of 4 GeV.

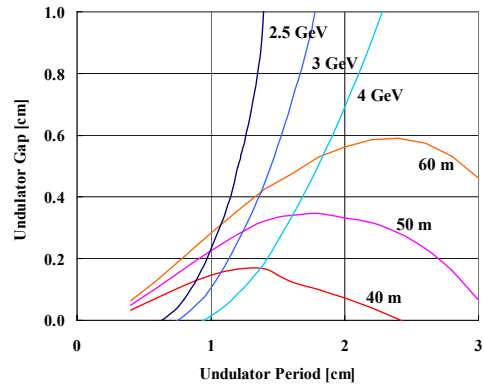


Figure 1: Undulator period and gap length for 0.3-nm SASE for saturation lengths (40, 50, 60 m) and beam energy (2.5, 3, 4 GeV).

Table 2 summarizes the FEL parameters for a 0.3-nm PAL XFEL. The undulator beta value is adjusted to obtain as short a saturation length as possible. Undulator saturation length is approximately 20 times the 3D gain length  $L_g$ . The peak brilliance of the PAL XFEL is  $10^{12}$  time higher than the U7 undulator radiation from the PLS 3<sup>rd</sup> generation storage ring. The hard X-ray spontaneous

radiation from the undulator of the PAL XFEL is also  $10^{10}$  times brighter than the synchrotron radiation from the PLS bending magnet.

Table 2: FEL parameters for 0.3-nm PAL XFEL

|  |        |
|--|--------|
| Undulator period [mm]                  | 12.5   |
| Undulator gap [mm]                     | 3.0    |
| Peak magnetic field [T]                | 0.97   |
| Undulator parameter, K                 | 1.14   |
| Beta [m]                               | 15     |
| 1D FEL parameter                       | 4.3e-4 |
| 1D gain length [m], $L_{1d}$           | 1.35   |
| 3D gain length correction, $\eta^*$    | 0.97   |
| 3D Gain length [m], $L_g$              | 2.67   |
| Effective FEL parameter                | 2.2e-4 |
| Cooperation length [nm]                | 63     |
| Saturation length [m]                  | 52     |
| Peak power [GW]                        | 2.1    |
| Peak brightness [ $\times 10^{32}$ ]** | 1.4    |

\*  $L_g = (1+\eta) L_{1d}$   
 \*\* photons/sec-mm<sup>2</sup>-mrad<sup>2</sup>-0.1%BW

Figure 2 shows 3D gain length correction and 3D gain length according to normalized emittance, which are calculated according to M. Xie [4]. An electron beam has to match the transverse phase space for a diffraction-limited photon beam to get the minimum 3D gain correction. The gain correction factor of the PAL XFEL is larger than the LCLS and the TESLA XFEL due to a rather large normalized emittance relative to the natural radiation emittance. However, due to the small periodic length of an undulator, the gain length is smaller than others. Therefore, it is possible to realize a compact X-ray FEL by using an in-vacuum undulator with small period and a low energy linear accelerator.

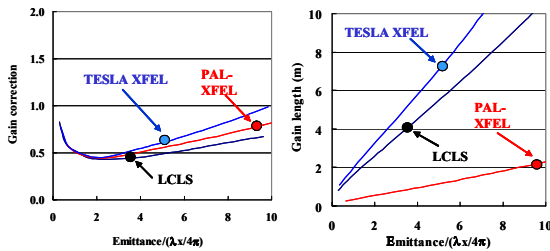


Figure 2: 3D gain correction factor and 3D gain length.

### XFEL LINAC DESIGN

The existing 2.5-GeV S-band PLS linac can be converted to X-ray FEL driver by adding a new S-band FEL injector linac. Figure 3 shows the layout of the PAL linac including a new undulator system. The FEL injector linac consists of a laser-driven photo-cathode gun, three S-band accelerating modules (X1, X2, X3), and two bunch compressors (BC1, BC2). The S-band photo-injector consists of a copper cathode and a 1.6-cell S-band RF cavity. The photoelectron beam is generated by 10-ps,

500-μJ, and 260-nm UV laser. It is accelerated to 7 MeV by a high gradient of 120 MV/m.

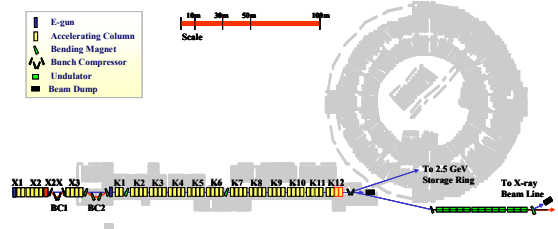


Figure 3: 3-GeV Linac for PAL XFEL.

The injector layout presented in FEL2003 is improved in this work [2]. Instead of the dog-leg layout, the new injector is aligned to the center line of the existing linac to suppress as far possible as emittance degradation due to CSR. All bunch compressors are included in the new injector area to preserve the existing layout of PLS 2.5-GeV linac. Figure 4 shows the layout of the new FEL injector linac and gives details of BC1 which is almost the same as the BC2 design. A suitable energy spread for bunch compression is provided by the modulator unit X2. The 4<sup>th</sup> harmonic cavity X2X linearizes the non-linear energy spread due to the RF curvature caused by the S-band modulator. The net chicane length is 12.2 m. The total chicane length becomes 17 m including focusing quadrupoles. The maximum beam offset in the middle of the bunch compressor is 33 cm.

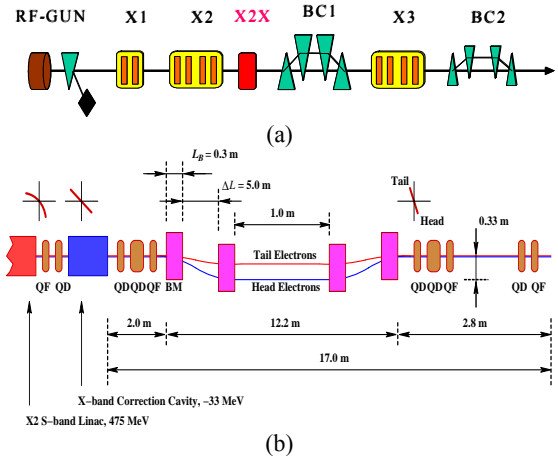


Figure 4: New injector layout (a) and details of BC1 (b).

The lattice design of two bunch compressors is shown in Fig. 5. The lattice is optimised by the following equation for the relative emittance growth [5]. The optimum condition is given at the alpha value of about 0 and beta function of about 3.

$$\frac{\Delta \varepsilon}{\varepsilon} = \sqrt{1 + \frac{(0.22)^2 \gamma_e^2 N^2}{36 \gamma \varepsilon_N \beta} \left( \frac{|\theta|^5 L_B}{\sigma_z^4} \right)^{\frac{2}{3}} [L_B^2 (1 + \alpha^2) + 9\beta^2 + 6\alpha\beta L_B]}$$

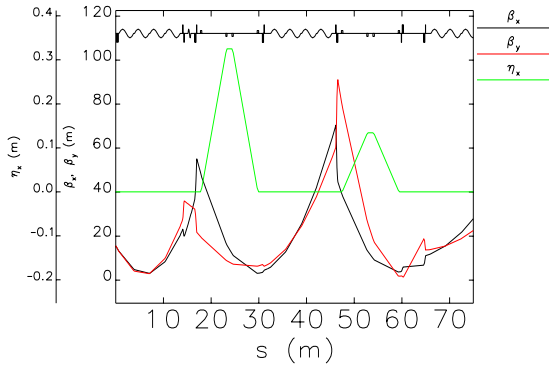


Figure 5: Lattice profile of two bunch compressors.

Against projected parameter dilution due to CSR and chromatic effect, adopted lattice design concepts are as follows: long drift space to reduce bending angle for a required R56, small bending angle at a large energy spread, large compression factor at BC1 and small compression factor at BC2. Strong focusing lattice around BCs to reduce CSR induced emittance growth, small quadrupole length around BCs to reduce the chromatic effects, smaller maximum beta-function of  $\sim 60$  m at the entrance of BC1, larger maximum beta-function at the entrance of BC2 after reducing energy spread are also effective. Against slice parameter dilution due to the micro-bunching instability, the following design concepts are adopted: normal 4-bend chicane instead of S-type chicane, large relative uncorrelated energy spread at BC2 by putting BC2 in the low energy region, no laser beam heater or superconducting wiggler. Table 3 shows the design parameters of the bunch compressor BC1 and BC2.

Table 3: Design parameters of bunch compressors

| Parameter               | BC1       | BC2       |
|-------------------------|-----------|-----------|
| BC type                 | Two stage | Two stage |
| Bending angle           | 3.50°     | 1.45°     |
| Momentum compaction R56 | 38.9 mm   | 6.70 mm   |
| Chicane length          | 12.2 m    | 12.2 m    |
| Dipole length           | 0.3 m     | 0.3 m     |
| Drift length $\Delta L$ | 5.0 m     | 5.0 m     |

### SIMULATION

We examined beam parameters using the ASTRA code from the photo-injector to the X1 booster unit considering strong space charge effects in this region. The code ELEGANT is used to design the main linac lattice from the X2 unit to the end of the existing linac. This code includes CSR effects in the bunch compressor and geometric wake field effects in the accelerating section. Table 4 summarizes the simulated beam parameters for BC1 and BC2. All uncorrelated energy spread is estimated at  $\pm 0.1$  mm core region. Initial uncorrelated energy spread at BC2 is increased after compression by

BC1. The uncorrelated energy deviation at BC2 is larger than the  $1 \times 10^{-5}$  that is required to suppress the micro-bunching instability.

Table 4: Beam parameters of bunch compressors

| Parameter                   | BC1                  | BC2                  |
|-----------------------------|----------------------|----------------------|
| Beam energy                 | 442 MeV              | 700 MeV              |
| Relative energy spread      | 1.84%                | 1.31%                |
| Uncorrelated energy spread  | $9.2 \times 10^{-6}$ | $4.3 \times 10^{-5}$ |
| Initial rms bunch length    | 820 $\mu\text{m}$    | 114 $\mu\text{m}$    |
| Final rms bunch length      | 114 $\mu\text{m}$    | 26 $\mu\text{m}$     |
| Compression factor          | 7.2                  | 4.38                 |
| Initial projected emittance | 0.90 $\mu\text{m}$   | 1.01 $\mu\text{m}$   |
| Final projected emittance   | 1.01 $\mu\text{m}$   | 1.12 $\mu\text{m}$   |

Figure 6 shows the energy spread and beam size before BC1 and at the end of the linac, respectively. The energy spread along the bunch length is well linearized by the X-band section (X2X) before BC1. At the entrance of BC1, energy spread is 1.835% and the beam size is 230  $\mu\text{m}$  ( $\sigma_x$ ). At the end of the linac the energy spread is 0.033% and beam size is 68.1  $\mu\text{m}$  ( $\sigma_x$ ). The longitudinal short-range wake-field damps the energy spread so that the energy spread becomes flatter and uniform.

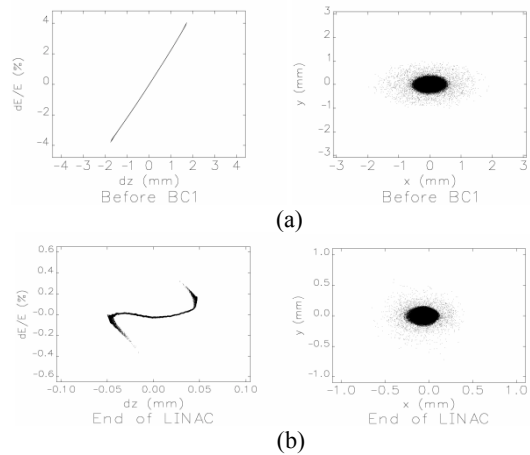


Figure 6: Energy spread and beam size before BC1 (a) and at the end of linac (b).

Figure 7 shows the variation of the projected energy spread and the bunch length along the linac. The relative energy spread is continuously increased to 1.84% until the entrance of BC1 by the modulator unit to fit the necessary compression factor at the BC1. The variation of energy spread in BC2 is mainly caused by CSR effects and kept reasonably low, which means the CSR is not so high in BC2. Increasing the beam energy, the energy spread is continuously decreased to 0.033% at the end of the linac. The large compression at BC1 and small compression at BC2 are clearly shown in the figure. The bunch length is compressed down to 26  $\mu\text{m}$  after BC2.

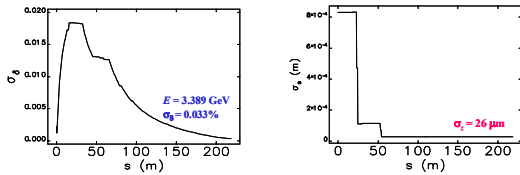


Figure 7: Energy spread and bunch length along linac.

Figure 8 shows the beam quality at the end of linac. The required beam parameters for FEL lasing at the undulator entrance correspond to dotted lines for the peak current of 4 kA, normalized emittance of 1.5  $\mu\text{m}$ , and energy spread of 0.02%. The normalized emittance, that is the most sensitive FEL parameter, is well below the requirement along the bunch, which gives reasonable margin for saturation within a 60-m long undulator. The lowest peak current along the bunch is about 20% less than 4 kA. The slice emittance is also 20% lower than the nominal value of 1.5  $\mu\text{m}$ . Because the saturation length is more sensitive to the emittance, it is possible to have saturation along the whole bunch.

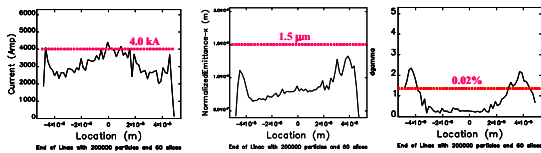


Figure 8: Beam quality at the end of linac.

## DISCUSSION

The bunch compressor design can be tuned to provide a suitable beam heating effect. Figure 9 shows the distribution of uncorrelated energy spread along the bunch length before BC1 and after BC1, respectively. The uncorrelated energy deviation within  $\pm 1.0$  mm bunch core is 4 keV at the entrance of BC1. It is increased to 30 keV at the entrance of BC2 due to the high compression factor at the BC1. Considering space charge forces, it will be increased further, which helps to suppress micro-bunching instabilities.

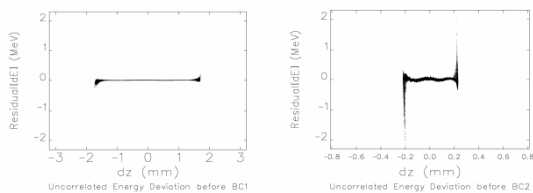


Figure 9: Uncorrelated energy spread at the entrance of BC1 and BC2.

In order to smoothly transfer the beam induced wall current, nickel foil, plated with copper, is attached on the pole surface using the magnetic attractive force. The practical smooth surface on commercially available metal plate has a high aspect-ratio of surface roughness, which

makes the energy spread due to the surface roughness negligibly small enough. The energy spread due to the resistive wake field on the electron beams in the undulator can be estimated by assuming the radius being equal to half of the gap and energy spread being half of the pipe radius [3]. With the bunch charge of 1-nC, and the gap size of 3 mm, undulator length of 60 m, the projected energy spread due to the resistive wall wake is 0.07% for the bunch length of 26  $\mu\text{m}$ . As the slippage length is 1.26  $\mu\text{m}$ , the contribution to the slice energy spread is negligible. The emittance growth due to transverse resistive wall wake is less than 1% if the random oscillation is kept less than 20  $\mu\text{m}$  with a Gaussian beam according to reference [6]. The gap size of each undulator can be tapered to adjust the resonant condition for the reduced average beam energy due to the incoherent synchrotron radiation loss.

The length of each undulator has to be at least  $2xL_g$  in order to release the tight tolerance of longitudinal and transverse misalignment [7]. The achievable radiation power is reduced to 50% if the phase slip is  $\pi$  over the drift section between the adjacent segments or the radiation is cut off at the drift section. As the saturation length is  $20xL_g$ , the maximum number of segments is 10 and the minimum length of an undulator is 6 m for the PAL XFEL.

The jitter and sensitivity analysis on the combined parameter space is extensively studied in reference [8]. It is still necessary to analyse the hardware upgrade scheme and the stability requirements with related technical parameters.

## ACKNOWLEDGMENTS

This work is supported by POSCO and the Ministry of Science and Technology (MOST) of Korea.

## REFERENCES

- [1] <http://pal.postech.ac.kr/>
- [2] J. S. Oh, et al., "0.3-nm SASE FEL at PAL," Nuclear Instruments and Methods in Physics Research A528, 582 (2004)
- [3] T. Shintake, et al., "SPRING-8 Compact SASE Source (SCSS)," in Proc. the SPIE2001, San Diego, USA, 2001; <http://www-xfel.spring8.or.jp>
- [4] M. Xie, "Design Optimization for an X-ray Free Electron Laser Driven by SLAC Linac," LBL Preprint No-36038, 1995
- [5] T. Limberg, "Emittance Growth in the LCLS due to Coherent Synchrotron Radiation," SLAC internal note, Oct. 1997
- [6] LCLS CDR, SLAC-R-593 (2002)
- [7] T. Tanaka, et al., "Misalignment effects of segmented undulator in self-amplified spontaneous emission," PRST-AB, 5(2002)040701
- [8] Y. Kim, et al., "Start-To-End Simulation of the PAL XFEL Project," 26<sup>th</sup> International FEL Conference and 11<sup>th</sup> FEL Users Workshop, Trieste, Italy, 2004